



# Impact of *Allium ursinum* Extract on the Metabolism of Diabetic Mice: An NMR-Based Approach to Uncover Glucose-Regulating Mechanisms

Zohreh Rahimi<sup>1</sup>, Zeynab Pezeshki<sup>1</sup>, Saeed Alinejad Moallem<sup>1</sup>, Fatereh Rezaei<sup>2</sup>, Taher Elmi<sup>3\*</sup>, Mostafa Akbariqomi<sup>4\*</sup>

<sup>1</sup> Department of Laboratory Sciences, Bab.C., Islamic Azad University, Babol, Iran

<sup>2</sup> Department of Biology, Bab.C., Islamic Azad University, Babol, Iran

<sup>3</sup> Department of Parasitology and Mycology, School of Medicine, Arak University of Medical Sciences, Arak, Iran

<sup>4</sup> Tissue Engineering and Regenerative Medicine Research Center, New Health Technologies Institute, Baqiyatallah University of Medical Sciences, Tehran, Iran

**Corresponding Author:** Taher Elmi, PhD, Assistant Professor, Department of Parasitology and Mycology, School of Medicine, Arak University of Medical Sciences, Arak, Iran. Tel: +989361117610, E-mail: [t.elmi@arakmu.ac.ir](mailto:t.elmi@arakmu.ac.ir); Mostafa Akbariqomi, PhD, Assistant Professor, Tissue Engineering and Regenerative Medicine Research Center, New Health Technologies Institute, Baqiyatallah University of Medical Sciences, Tehran, Iran. Tel: +9887554832, E-mail: [makbariqomi@gmail.com](mailto:makbariqomi@gmail.com)

Received September 27, 2025; Accepted November 9, 2025; Online Published March 30, 2026

## Abstract

**Introduction:** *Allium ursinum* (*A. ursinum*) is a medicinal plant recognized for its wide range of therapeutic properties, including anti-inflammatory, antioxidant, and antidiabetic activities. Nevertheless, the precise metabolic mechanisms underlying antidiabetic effects remain insufficiently understood. In this study, we aimed to investigate the hypoglycemic effects of *A. ursinum* hydro-methanolic extract and characterize the associated metabolic changes in diabetic Balb/C mice.

**Materials and Methods:** Hydro-methanolic extract of *A. ursinum* was prepared, and then its polar and volatile constituents were identified using Liquid Chromatography-Mass Spectrometry and Gas Chromatography-Mass Spectrometry, respectively. Forty mice were allocated into control groups (healthy, diabetic + solvent, and diabetic + metformin) and experimental groups receiving different doses of *A. ursinum* extract. Treatments were administered for 21 consecutive days, after which blood glucose levels were assessed, and the effective doses (ED<sub>50</sub> and ED<sub>90</sub>) were calculated. To assess metabolic changes associated with the hypoglycemic effects, serum samples were analyzed using proton nuclear magnetic resonance (<sup>1</sup>H-NMR)-based metabolomics. Hepatic and renal toxicity were evaluated by enzymatic assay and histopathological examinations.

**Results:** The administration of *A. ursinum* at tested doses led to a significant decrease in blood glucose levels in diabetic mice (160 mg/kg). These hypoglycemic effects were accompanied by notable changes in the serum metabolic profile, affecting pathways such as ketone body synthesis and degradation, D-glutamate metabolism, pyruvate metabolism, glycolysis/gluconeogenesis, arginine biosynthesis, and the tricarboxylic acid cycle. Importantly, no evidence of liver or kidney toxicity was observed at the higher dose (ED<sub>90</sub> = 141 mg/kg).

**Conclusions:** This study showed that *A. ursinum* has antidiabetic effects and highlighted the role of metabolite changes in diabetes pathophysiology. Hence, the glucose-lowering metabolites identified could be potential targets for the development of future antidiabetic treatments.

**Keywords:** Plant Extract, *Allium ursinum*, Metabolomics, Diabetes, Hypoglycemic, Tissue Toxicity

**Citation:** Rahimi Z, Pezeshki Z, Alinejad Moallem S, Rezaei F, Elmi T, Akbariqomi M. Impact of *Allium ursinum* Extract on the Metabolism of Diabetic Mice: An NMR-Based Approach to Uncover Glucose-Regulating Mechanisms. J Appl Biotechnol Rep. 2025;13(1):1940-1952. doi:10.30491/jabr.2025.549652.1922

## Introduction

Diabetes is a chronic and heterogeneous disease characterized by metabolic disturbances in carbohydrates, lipids, and proteins. The primary biochemical marker of this disease is chronic hyperglycemia, which results from either relative or complete insulin deficiency. Individuals with diabetes often experience severe complications, including cardiovascular and renal disorders, vision impairment, limb amputations due to neuropathy, and behavioral abnormalities.<sup>1</sup> At the molecular level, diabetes induces oxidative stress and

the production of free radicals, which lead to mitochondrial lipid, protein, and DNA oxidation. Furthermore, disruptions in metabolic pathways contribute to impaired DNA function.<sup>2,3</sup> The common diabetes treatment, insulin, can cause skin lesions in some patients.<sup>4</sup> Moreover, although rare, some diabetic individuals exhibit immediate allergic reactions to insulin, such as urticaria, angioedema, and hypotension following injection.<sup>5</sup> Given these challenges, researchers have increasingly explored the use of herbal

extracts as a means to mitigate diabetes-induced damage.

Epidemiological studies suggest that incorporating certain plant species, particularly those from the *Allium* genus, into the diet can significantly improve diabetes management, blood lipid profiles, and blood pressure regulation.<sup>6-8</sup> Iran, with its suitable geographical and climatic conditions, is home to various plant species, including *Allium ursinum* (*A. ursinum*), whose therapeutic efficacy has been well-documented. This plant exhibits antibacterial and antioxidant activity due to its high content of cysteine sulfoxides and sulfonic acid amino acids.<sup>9,10</sup>

To identify the mechanism of a drug's effect on disease progression, various methods are available, such as hydrogen-1 nuclear magnetic resonance (<sup>1</sup>H-NMR) spectroscopy. Through <sup>1</sup>H-NMR, we can identify metabolite changes in serum that may distinguish between diabetic and healthy individuals.<sup>11</sup> Targeting differentially expressed metabolites offers new opportunities for disease management. By disrupting the genes responsible for producing key metabolic intermediates, it may be possible to halt disease progression without relying on broad-spectrum drugs with high toxicity. This approach offers the potential for targeted treatments in the near future.<sup>12</sup> Using <sup>1</sup>H-NMR spectroscopy coupled with chemometric modeling, it is possible to identify chemical reactions within cells and compare metabolites across different therapeutic phases to identify specific markers.<sup>13</sup> A major advantage of metabolomics over other methods is its ability to analyze metabolites in a simultaneous, network-based manner, providing a comprehensive understanding of their relationships.<sup>14</sup>

Given the challenges associated with the treatment of diabetic complications, finding an effective drug with minimal side effects remains crucial. *A. ursinum* is considered a promising candidate for diabetes management. Several studies have highlighted its potential in modulating blood glucose levels and enhancing insulin sensitivity. However, the precise metabolic mechanisms underlying these effects remain unclear. In this study, we evaluated the hypoglycemic effect of hydro-methanolic *A. ursinum* extract in diabetic Balb/C mice and employed NMR-based metabolomics to characterize associated metabolic alterations. This approach aims to identify key metabolic pathways involved in blood glucose reduction and provide a deeper understanding of the biochemical processes influenced by *A. ursinum*, ultimately contributing to the development of more targeted and effective antidiabetic therapies.

## Materials and Methods

### Studying and Describing the Plant's Features

#### Plant Materials

The plant material was collected in the spring from Alborz Province, Iran, at an altitude of 200 to 500 meters along the Chalus Road region. The bulb and aerial parts of the plant

were separated and air-dried in a shaded area to preserve them properly. The plant specimen was identified and authenticated by the Department of Biology at Azad University.

#### Extraction of the Plant

The hydro-methanolic extract of *A. ursinum* was prepared using the percolation method.<sup>15</sup> The dried plant material was finely ground and mixed with a methanol-water solution (4:1 ratio) in an Erlenmeyer flask. The flask was covered with aluminum foil to prevent light exposure. The mixture was stirred for 30 minutes on an electric shaker and then allowed to macerate in the dark for 24 hours. The extract was filtered through filter paper, and the solvent was removed by rotary evaporation to concentrate the extract. The concentrated extract was then freeze-dried to obtain the lyophilized powder. The stock solution was prepared by dissolving an appropriate amount of the lyophilized powder in normal saline and dimethyl sulfoxide (DMSO 0.5%).

#### Liquid Chromatography-Mass Spectrometry (LC-MS)

To detect polar and non-volatile compounds in *A. ursinum* that are stable at high temperatures, LC-MS was employed (Agilent 1200 HPLC system with Diode Array Detection, coupled to an Agilent 6110 single quadrupole mass spectrometer). Compound separation was achieved using an Eclipse XDB C18 column (4.6 × 150 mm, 5 μm particle size) from Agilent Technologies (Santa Clara, CA, USA) at ambient temperature. The mobile phases consisted of 0.1% acetic acid/acetonitrile (99:1, v/v) in distilled water and 0.1% acetic acid in acetonitrile (v/v). The elution flow rate was set to 0.5 ml/min. Spectra of the compounds were recorded between 200 and 600 nm, and the molecular scan range was from 100 to 1000 m/z. Chromatograms specific to phenolic acids (280 nm) and flavonols (340 nm) were also analyzed.

#### Gas Chromatography-Mass Spectrometric Analysis (GC-MS)

To identify volatile and low-molecular-weight organic compounds in *A. ursinum*, the Agilent 6890N GC-MS system was employed. The gas chromatography temperature program was set as follows: starting at 40 °C for 5 minutes, increasing at a rate of 5 °C/min to 200 °C (maintained for 5 minutes), then raised at 10 °C/min to a final temperature of 280 °C (held for 10 minutes). Pure helium was used as the carrier gas at a constant flow rate of 1 ml/min. A high ionization energy of 69.9 eV was applied, with a fragment scan range of 40 to 550 m/z.<sup>16</sup>

#### In Vivo Experiments

##### Experimental Animals

Male BALB/c mice of similar age were housed in groups of five in the animal facility, maintained under a 12-hour

light/dark cycle, and kept at a temperature range of 22-25 °C. Animal handling procedures were conducted following the standard approved methods set by the Ethics Committee of the Islamic Azad University, Babol Branch, Iran.

The diabetic mouse model was induced by feeding a high-fat, high-sucrose diet followed by the injection of streptozotocin (STZ, dissolved in 0.1 M citrate buffer, pH 4.5) at a dose of 45 mg/kg.<sup>17</sup> Fasting blood glucose levels were measured on days 2 and 9 to confirm the induction of diabetes. Mice with fasting blood glucose levels greater than 200 mg/dl were classified as diabetic, while those with lower levels underwent a second injection. Blood glucose levels were measured using a Roche Glucometer (Accu-Chek, Roche, Germany).

### *Hypoglycemic Effect of A. ursinum*

The study involved forty male mice divided into control and experimental groups. The control group had three subgroups: healthy mice that did not receive any treatment (survival group), diabetic mice treated with extraction solvent (PBS+DMSO) as a negative control, and diabetic mice treated with metformin (500 mg/kg) as a positive control. The experimental group had five subgroups of diabetic mice given different doses (10, 20, 40, 80, and 160 mg/kg) of *A. ursinum* plant extract for 21 consecutive days. Blood samples were collected on the final day via heart puncture. The serum was then separated, and blood glucose levels were measured. The effective doses (ED<sub>50</sub> and ED<sub>90</sub>) of plant extract on blood glucose levels in diabetic mice were determined using non-linear regression analysis with PRISM software, version 9.

### *Serum Metabolic Changes in Mice*

After determining the ED<sub>50</sub>, 10 mice were randomly divided into control and experimental groups. The control group included 5 diabetic mice receiving solvent, while the experimental group comprised 5 diabetic mice receiving the ED<sub>50</sub> dose of the plant extract. After the treatment period, the mice were anesthetized with a ketamine/xylazine combination, and blood samples were collected via heart puncture. The serum was separated and prepared for metabolite extraction, then sent to a laboratory equipped with a <sup>1</sup>H-NMR spectrometer for analysis.<sup>13</sup> The serum samples were individually placed in NMR probes for <sup>1</sup>H-NMR spectroscopy using the CPMG pulse sequence. TSP served as the internal standard with a chemical shift of zero. Each sample underwent 150 scans lasting 15 minutes each. Following spectroscopic analysis, the spectra of the 10 samples were processed using computational methods. The resulting metabolomic data, containing thousands of signals and providing a comprehensive overview of the metabolic profile under specific biological conditions, were converted into a suitable format for further analysis using ProMetab

software, a metabolomic data processing tool. Partial Least Squares Discriminant Analysis (PLS-DA) was conducted using MetaboAnalyst 6.0 (<https://www.metaboanalyst.ca>). Subsequently, chemical shifts were identified, and the significant metabolites were determined using the Human Metabolome Database (<https://www.hmdb.ca>).

### *Toxicity Test*

Fifteen mice were randomly divided into control and experimental groups for toxicity testing. The control group had two subgroups: one received solvent as a negative control and the other received metformin as a positive control. In contrast, the experimental group received the ED<sub>90</sub> dose of the plant extract for 21 consecutive days.

### *Body Weight Assessment in Mice*

During the treatment period, the body weight of the mice was measured on the first and last days and compared to the negative control group. To minimize external influences, the mice were housed individually in separate cages. Each mouse's weight was measured using a precise digital scale. All procedures were conducted under standardized and controlled conditions and close supervision to ensure the reliability and consistency of the results. Weight variations from day 1 to day 21 were analyzed to assess the therapeutic impact and identify any possible side effects.

### *Enzymatic Assay*

After the 21-day treatment period, the mice were euthanized under anesthesia induced by a ketamine/xylazine mixture. Blood samples were collected through cardiac puncture to analyze red blood cell morphology and assess serum levels of aspartate aminotransferase (AST), alanine aminotransferase (ALT), and alkaline phosphatase (ALP). The blood samples were centrifuged at 3000 rpm for 15 minutes to separate the serum from the formed clot. AST activity was measured using a biochemical kit from CO BioChem (Lot no. 92003), ALT activity with a separate kit from the same company (Lot no. 92005), and ALP levels with another kit from CO BioChem (Lot no. 92005). All assays adhered to the International Federation of Clinical Chemistry (IFCC) guidelines and were conducted using the COBAS MIRA analyzer.

### *Histopathological Analysis*

Following blood collection and euthanasia, the mice were dissected to extract the liver and kidneys from the abdominal cavity. The tissues were washed with saline and fixed in 10% formalin. After 72 hours of fixation, thin sections (5 µm) were sliced using a rotary microtome, mounted in paraffin, and stained with hematoxylin and eosin (H&E). The stained sections were examined under a microscope to assess tissue damage, including cell degeneration, necrosis,

and inflammatory responses. Images of the slides were captured for documentation and analysis of histopathological alterations.

### Statistical Analysis

The data on the effect of the plant extract on blood glucose levels were analyzed using SPSS version 22 software. The data were expressed as means  $\pm$  standard deviations and tested for normality with the Kolmogorov-Smirnov test, confirming normal distribution. One-way ANOVA was conducted, followed by a post-hoc Tukey's test for pairwise comparisons. The level of  $p$ -values  $\leq 0.05$  was considered statistically significant.

## Results

### LC-MS and GC-MS Analysis

The composition and concentration of each phenolic compound in the *A. ursinum* extract were individually identified through LC-MS analysis. Seven compounds, including phenolic acids and flavonoids, were identified in the extract (Table 1). The identification process involved comparing co-elution times, mass spectra, and reference standards to confirm the identity of each compound.

**Table 1.** Major Compounds Identified and Quantified in *Allium ursinum* Extracts Using LC-MS

No	Time	Identification
1	3.12	Coumaric acid
2	3.36	Sinapic acid
3	3.88	Ferulic acid
4	10.78	Syringic acid
5	15.34	Kaempferol 3-(6''-acetyl)glucoside)
6	18.72	Kaempferol O-glucoside
7	20.19	Kaempferol

The GC-MS chromatogram revealed the presence of 39 major compounds in the hydro-methanolic extract of *A. ursinum*. Some notable organic compounds identified were propenyl disulfide, methyl-2-propenyl disulfide, vinyl-1,3-dithiane, propionic acid, and furfural. These compounds were identified by comparing their retention times, peak

areas (%), peak heights (%), and spectral fragmentation patterns with known compounds in the National Institute of Standards and Technology (NIST) library (Table 2).

**Table 2.** The Most Phytochemical Constituents Identified in the Hydro-Methanolic Extract of *Allium ursinum* Using GC-MS (in % of total ion current).

No.	Compounds	% Of total
1	Methyl-2-propenyl disulfide	4.6
2	Propenyl propyl disulfide	1.8
3	di-2-Propenyl trisulfide	3.7
4	Vinyl-4H-1,3-dithiine	3.2
5	di-2-Propyl trisulfide	4.1
6	Propylene sulfide	0.8
7	Decanal	1.3
8	Heptacosane	0.7
9	Tricosane	0.9
10	Furfural	0.4
11	Hexacosane	0.5
12	Nonacosane	0.3
13	Benzaldehyde	2.8
14	Diallyl trisulphide	4.8
15	Ethene, 1-(ethylthio)	0.4

### Hypoglycemic Activity of *A. ursinum* Extract

Table 3 presents the hypoglycemic effect of the hydro-methanolic extract of *A. ursinum* at concentrations of 10, 20, 40, 80, and 160 mg/kg on streptozotocin-induced diabetic mice, compared to the control groups. The results showed that oral administration of *A. ursinum* extract at doses of 160 and 80 mg/kg significantly reduced blood glucose levels in diabetic mice, compared to the negative control groups, from 388 mg/dl to 116 mg/dl and 191 mg/dl, respectively ( $p < 0.01$ ). Notably, the average reduction in blood glucose levels in the group treated with the 160 mg/kg extract was greater than that observed in the group treated with metformin as a positive control. However, this difference was not statistically significant ( $p = 0.984$ ).

The ED<sub>50</sub> value (the effective dose of the extract that reduces blood glucose levels by 50%) and the ED<sub>90</sub> value (the effective dose of the extract that reduces blood glucose levels by 90%) were calculated to be 55 mg/kg and 141 mg/kg, respectively using GraphPad Prism version 9 software (Figure 1).

**Table 3.** Blood Glucose Levels of the STZ-Induced Diabetic Groups and the Control Groups

Groups	Subgroups	Blood glucose (mg/dl) (Mean $\pm$ SE)
Experimental ( <i>Allium ursinum</i> )	10 mg/kg	386.2 $\pm$ 3.9 <sup>a</sup>
	20 mg/kg	367.6 $\pm$ 6.1 <sup>a</sup>
	40 mg/kg	285.2 $\pm$ 3.2 <sup>b</sup>
	80 mg/kg	191.4 $\pm$ 4.7 <sup>c</sup>
	160 mg/kg	116 $\pm$ 7.7 <sup>de</sup>
Control	Survival	97.2 $\pm$ 5.3 <sup>e</sup>
	Negative (Solvent)	388.8 $\pm$ 5.3 <sup>a</sup>
	Positive (Metformin)	122.6 $\pm$ 3.4 <sup>d</sup>

### Impact of *A. ursinum* Extract on the Metabolites of Mice Analysis of Metabolic Pathways

Initially, the <sup>1</sup>H-NMR spectra were normalized, and the data were subsequently analyzed using Partial Least Squares Discriminant Analysis (PLS-DA) (Figure 2). Volcano plots

were generated to visualize the data based on magnitude, and differential metabolites were identified through multivariate statistical analysis (Figure 3). The analysis showed statistically significant differences in the metabolic pathways of diabetic mice treated with the ED<sub>50</sub> dose of *A. ursinum* extract compared

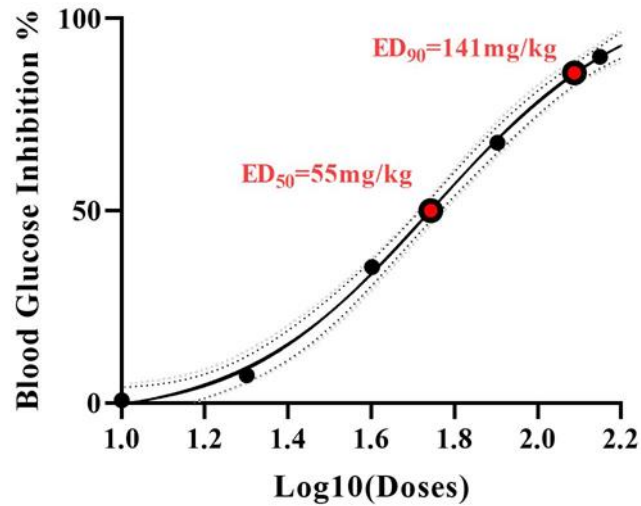


**Figure 1.** The Effective Doses of *Allium ursinum* Plant Extract on Blood Glucose Levels in Diabetic Mice Based on ED50 and ED90.

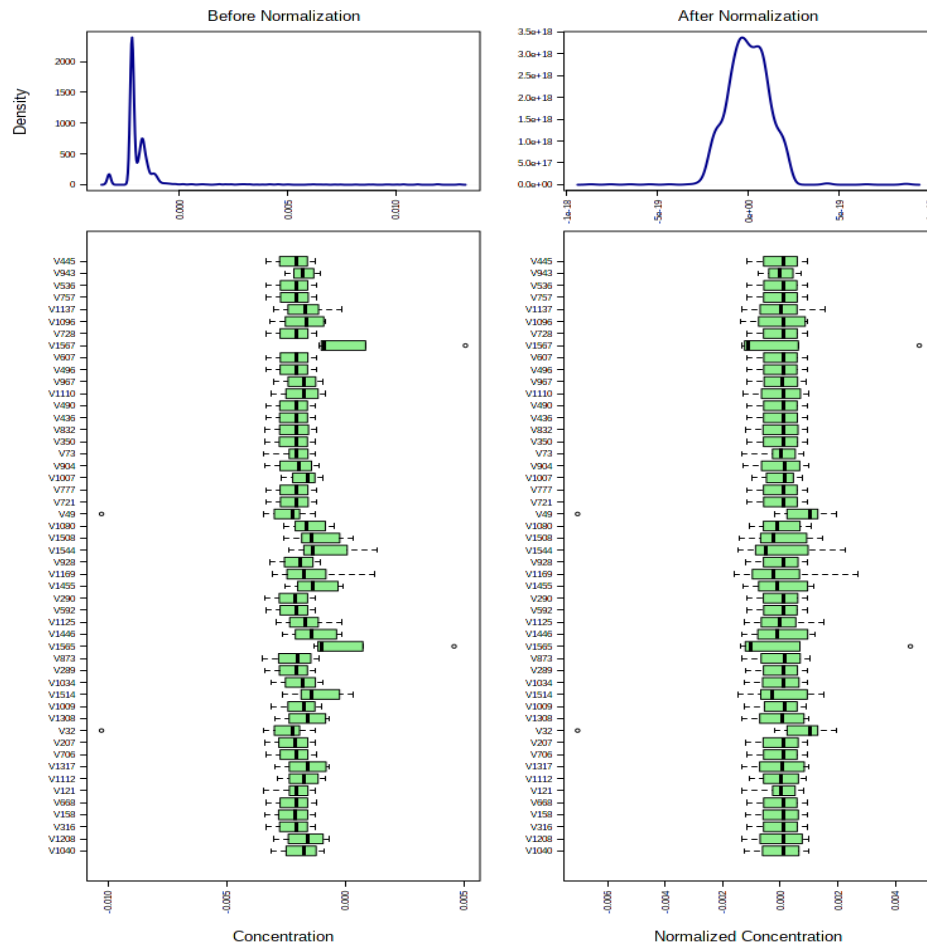


**Figure 2.** Normalization of Spectra Using the MetaboAnalyst Software. Spectral data obtained from the analysis are first processed to account for variations due to experimental conditions, such as sample concentration and instrument calibration. The normalization procedure standardizes the intensity values across all spectra, enabling accurate comparisons between samples. This step is crucial for eliminating systematic biases and ensuring the reliability of downstream analyses.

to those receiving solvent (Table 4). These changes were primarily observed in the synthesis and degradation of ketone bodies, D-glutamine and D-glutamate metabolism,

pyruvate metabolism, glycolysis/ gluconeogenesis, arginine biosynthesis, and the citrate cycle pathway (Figure 4). In Table 4, "Total" refers to the number of compounds involved

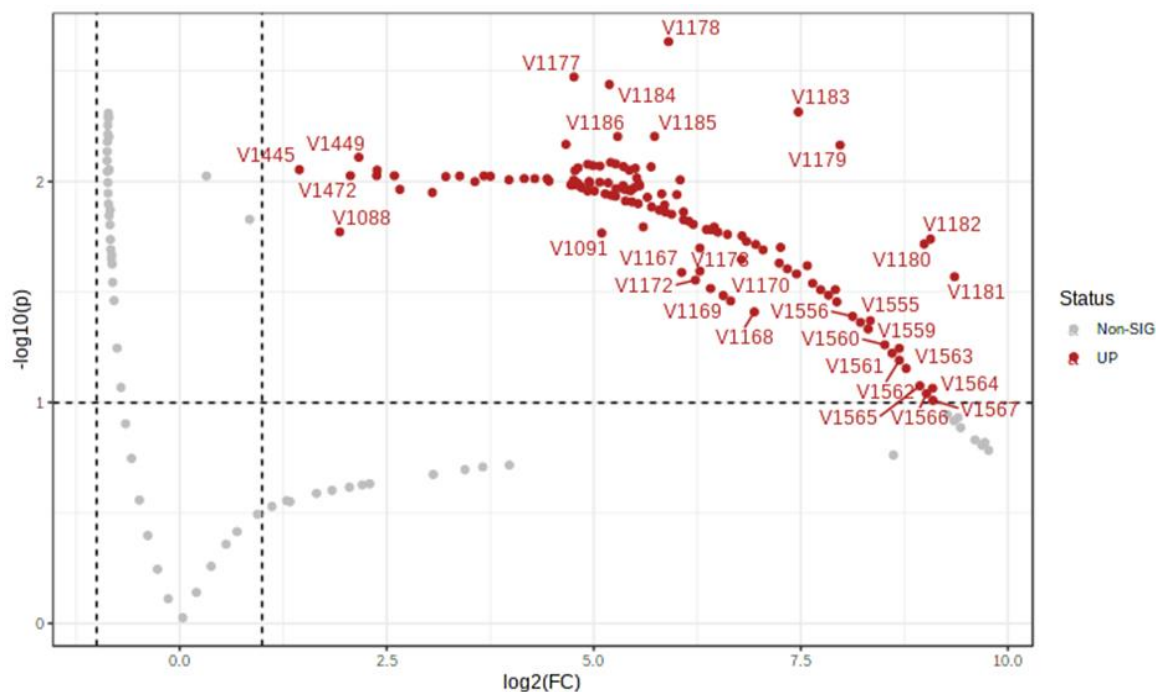


**Figure 3.** Volcano Plots of Strain-Wise t-test of the Untargeted NMR Data. Metabolites significant after FDR correction are colored red (indicating an increase). The x-axis represents the fold-change in metabolite levels between different groups, while the y-axis shows the statistical significance ( $-\log_{10}$  p-value) of each metabolite. Metabolites that are statistically significant after False Discovery Rate (FDR) correction are highlighted in red, indicating a significant increase in their abundance in one group relative to the others. The volcano plot allows for the identification of differentially expressed metabolites with both large fold-changes and high statistical significance.

**Table 4.** Differentiating Metabolites and Pathways in the Control and Treated Groups with  $EC_{50}$  Dose of *Allium ursinum*

	Impact	FDR	Holm P	$-\log(p)$	Raw P	Hits	Expected	Total
Butanoate metabolism	0.11111	0.00336	0.00336	4.3985	4.00E-05	3	0.07742	15
Synthesis and degradation of ketone bodies	0.6	0.00702	0.01921	3.6356	0.00023	2	0.02581	5
Alanine, aspartate and glutamate metabolism	0.19712	0.00702	0.02285	3.5549	0.00028	3	0.14452	28
Nitrogen metabolism	0	0.00702	0.02805	3.4606	0.00035	2	0.03097	6
Glyoxylate and dicarboxylate metabolism	0.03175	0.00702	0.03342	3.3791	0.00042	3	0.16516	32
Citrate cycle (TCA cycle)	0.13672	0.05922	0.33414	2.3737	0.00423	2	0.10323	20
Glycine, serine and threonine metabolism	0.00958	0.13637	0.88638	1.9445	0.01136	2	0.17032	33
Arginine and proline metabolism	0.086	0.15681	1	1.8258	0.01494	2	0.19613	38
Tyrosine metabolism	0	0.16895	1	1.7423	0.0181	2	0.21677	42
D-Glutamine and D-glutamate metabolism	0.5	0.25721	1	1.514	0.03062	1	0.03097	6
Arginine biosynthesis	0.11675	0.53583	1	1.1539	0.07017	1	0.07226	14
Histidine metabolism	0	0.55882	1	1.0978	0.07983	1	0.08258	16
Pyruvate metabolism	0.20684	0.69977	1	0.96538	0.1083	1	0.11355	22
Glycolysis / Gluconeogenesis	0.10044	0.76106	1	0.89673	0.12684	1	0.13419	26
Glutathione metabolism	0.01966	0.76152	1	0.86649	0.13599	1	0.14452	28
Porphyrin and chlorophyll metabolism	0	0.76152	1	0.83848	0.14505	1	0.15484	30
Cysteine and methionine metabolism	0	0.78312	1	0.8	0.15849	1	0.17032	33
Valine, leucine and isoleucine degradation	0	0.88259	1	0.72325	0.18913	1	0.20645	40
Aminoacyl-tRNA biosynthesis	0	0.98563	1	0.65181	0.22294	1	0.24774	48

The columns indicate the impact of each metabolic pathway (Impact), False Discovery Rate (FDR), Holm  $p$ -value,  $-\log(p)$ , raw  $p$ -value, number of significant metabolites (Hits), the expected number of metabolites (Expected), and the total number of metabolites (Total). These data were collected to identify and analyze significant differences in metabolites and metabolic pathways in response to treatment with a specific dose of wild garlic (*Allium ursinum*).

in each pathway, while "Raw P" denotes the  $p$ -value calculated from the enrichment analysis.

### Identified Metabolic Changes

Metabolic pathways identified at the  $ED_{50}$  concentration of *A. ursinum* included metabolites obtained from the Human

Metabolome Database (HMDB) (<http://www.metabolomics.ca>) such as NADH, hydroxocobalamin, citric acid, acetoacetic acid, carbon dioxide, L-glutamic acid, 3-hydroxybutyric acid, and pyruvic acid (Table 5). In certain metabolic pathways, it was observed that a metabolite could shift between distinct metabolic routes, exhibiting varying levels

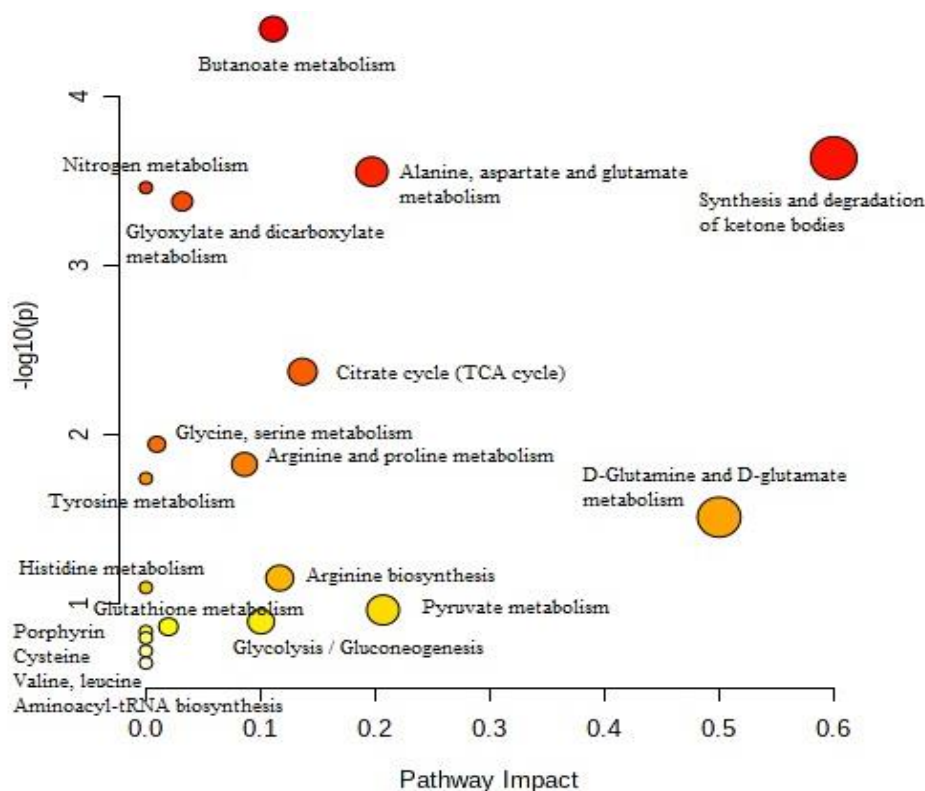


**Figure 4.** Summary of Pathway Analysis. Circles that are higher, bigger, and closer to the x-axis are more significant. The size, height, and proximity of the circles to the x-axis indicate the significance of each pathway. Larger, higher, and closer circles to the x-axis are considered more significant. This visual representation helps highlight the most impactful pathways in the dataset based on statistical significance.

**Table 5.** Metabolites with their ID were Identified from the Human Metabolome Database

NO.	Metabolite	HMDB	PubChem	KEGG	Flux
1	Acetoacetic acid	HMDB0000060	96	C00164	↑
2	Citric acid	HMDB0000094	311	C00158	↑
3	Hydroxocobalamin	HMDB0014345	44475014	C08230	↓
4	NADH	HMDB01487	928	C00004	↓
5	Pyruvic acid	HMDB0000243	1060	C00022	↑
6	3-Hydroxybutyric acid	HMDB0000357	441	C01089	↑
7	L-Glutamic acid	HMDB00148	33032	C00025	↓
8	Carbon dioxide	HMDB01967	280	C00011	↑

The red and green arrow indicates the increasing and decreasing the level of metabolite compare to negative control groups, respectively.

between the control and experimental groups (Figure 5).

### Toxicity Assay Results

There were no significant changes in body weight observed before and after the 21-day treatment in any experimental group compared to the negative control, as shown in Figure 6.

Table 6 shows that the serum levels of liver enzymes AST, ALT, and ALP in the experimental group (mice receiving the *A. ursinum* plant extract at the ED<sub>90</sub> dose) were similar to those in the negative control group (mice receiving solvent), with no significant difference between the two

groups ( $p > 0.05$ ). However, the levels of liver enzymes in mice receiving metformin (positive control) were significantly higher compared to both the ED<sub>90</sub> and negative control groups ( $p < 0.05$ ).

The analysis of liver tissue slides stained with H&E supported the enzymatic assay results. The liver in the group treated with the effective dose of the plant extract appeared normal, similar to the negative control group. In contrast, the metformin-treated group showed inflammatory cells and necrosis in the hepatic sinusoids. Kidney tissue in all groups appeared normal and was comparable to that of the negative control group (Figure 7).

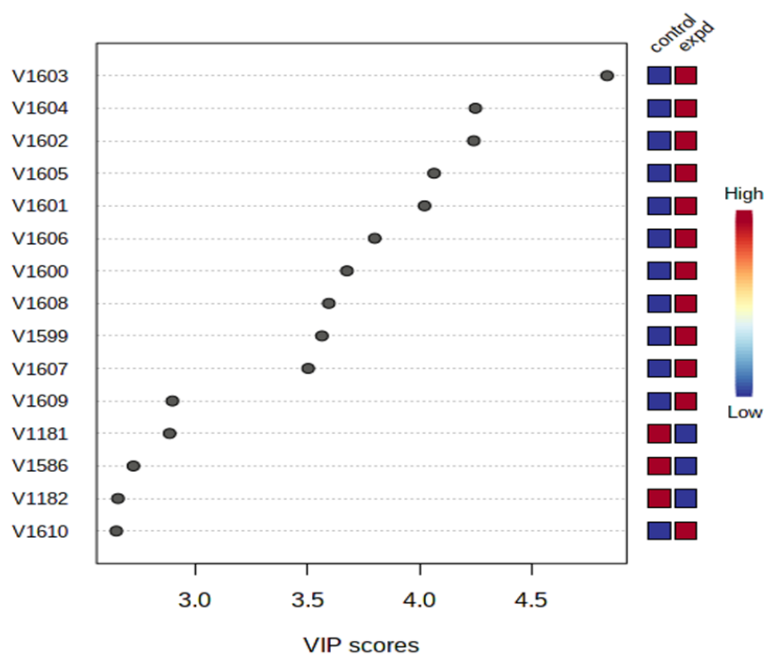


**Figure 5.** Important Features Identified by PLS-DA. VIP scores show the chemical shifts of the metabolites in the test group, indicated in blue (decrease in metabolites) and red (increase in metabolites).

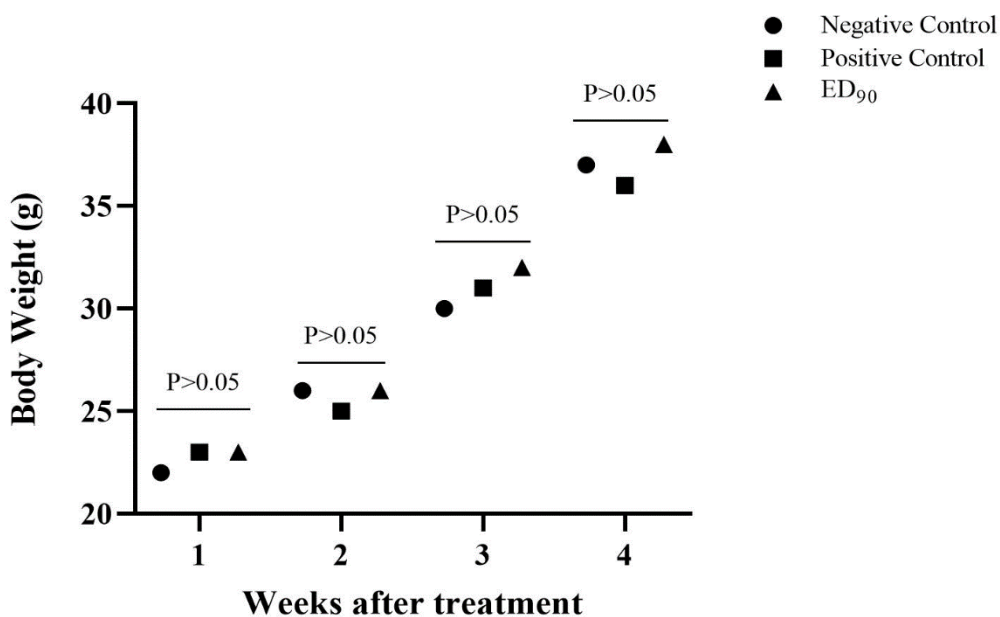


**Figure 6.** Body Weight Comparison of Mice after the Experimental Period ( $p < 0.05$  considered statistically significant).

**Table 6.** ALT, AST, and ALP Levels (U/L) in Plasma of Mice Treated with *Allium ursinum*

Groups	Subgroups	Serum enzyme (Mean $\pm$ SE)		
		ALT (U/L)	AST (U/L)	ALP (U/L)
Experimental ( <i>Allium ursinum</i> )	ED <sub>90</sub>	71.0000 $\pm$ 3.53 <sup>a</sup>	82.6000 $\pm$ 4.82 <sup>a</sup>	120.800 $\pm$ 5.26 <sup>a</sup>
Control	Negative (Solvent)	63.6000 $\pm$ 6.80 <sup>a</sup>	76.4000 $\pm$ 3.71 <sup>a</sup>	113.2000 $\pm$ 3.42 <sup>a</sup>
	Positive (Metformin)	97.0000 $\pm$ 5.24 <sup>b</sup>	97.0000 $\pm$ 6.04 <sup>b</sup>	164.2000 $\pm$ 7.88 <sup>b</sup>

Similar letters indicate no significant difference ( $p > 0.05$ ), and dissimilar letters indicate a significant difference ( $p \leq 0.05$ ) between different groups.

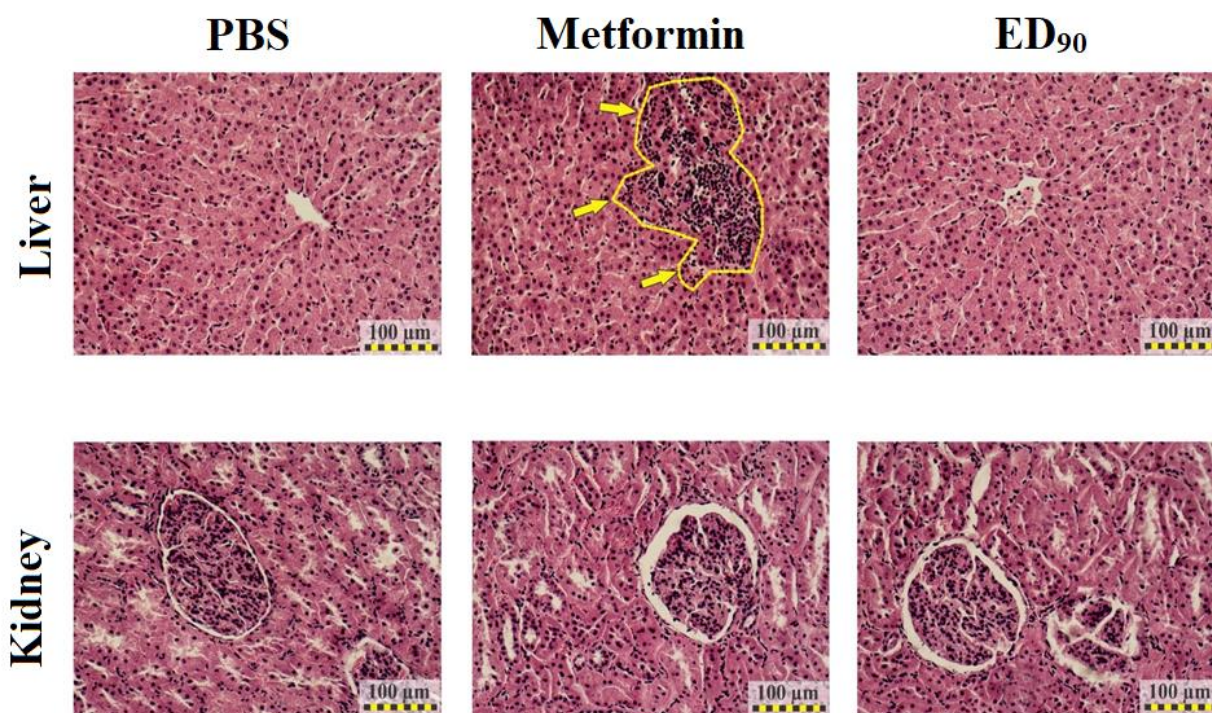


**Figure 7.** Histological Sections of Mice Liver and Kidney Tissues from the Negative Control Receiving Solvent, the Positive Control Receiving Metformin, and the ED<sub>90</sub> Dose Group of *Allium ursinum* Extract, Stained with Haematoxylin-Eosin. The yellow arrow indicates the accumulation of inflammatory cells and necrosis.

## Discussion

*A. ursinum*, commonly known as wild garlic, is a medicinal and edible plant recognized for its broad range of therapeutic properties, including anti-cancer,<sup>19</sup> anti-microbial, anti-parasitic, anti-inflammatory, cytotoxic, heart-protective,<sup>20</sup> antioxidant,<sup>21</sup> and anti-diabetic effects. Additionally, it has been reported to lower blood serum cholesterol levels by inhibiting cholesterol synthesis. A study by Tudu et al. (2022) confirmed that *A. ursinum* is effective in treating cardiovascular diseases, rheumatism, high blood pressure, liver diseases, and diabetes. This aligns with the anti-diabetic effects observed in our study.<sup>22</sup>

The beneficial properties of *A. ursinum* are attributed to its phytochemical constituents present in the extract. The main phytochemical compounds identified include phenolic acids, flavonoids, methyl-2-propenyl disulfide, propenyl propyl disulfide, di-2-propenyl trisulfide, vinyl-4H-1,3-dithiine, di-2-propyl trisulfide, and propylene sulfide, which were confirmed through LC-MS and GC-MS analysis in this study. Research by Sobolewska et al. and Sendl et al. showed that vinyl dithiins are cyclic compounds formed by the breakdown of allicin. These reaction products are typically found in less polar solvents, such as hexane or 2-propanol. Sulfides, which are volatile and stable, are responsible for the characteristic odor following garlic consumption. Additionally, polysulfides, as identified in our GC-MS results, are potent antioxidants.<sup>20,23</sup> It is noteworthy that several of the identified compounds exhibit well-

documented biological activities that are likely responsible for the observed effects of the extract. Specifically, phenolic acids (such as caffeic and chlorogenic acids) and flavonoids (such as quercetin and catechin) are widely recognized for their potent antioxidant and antimicrobial properties. In addition, sulfur-containing compounds detected through GC-MS analysis, including propenyl disulfide and methyl-2-propenyl disulfide, have been reported to possess strong antimicrobial and cytoprotective activities. Collectively, these groups of compounds are presumed to be the principal contributors to the overall bioactivity of the extract. Future investigations will include quantitative analyses aimed at elucidating the relative contribution of each compound class to the observed biological effects.

Other studies have shown that, in addition to *A. ursinum* extract, other plants such as ginger and *Allium schoenoprasum* also exhibit efficacy in lowering blood glucose levels. Fadil et al. found that the alcoholic extract of garlic and ginger at a dose of 500 mg/kg effectively reduced blood glucose levels and restored C-peptide levels in diabetic mice.<sup>24</sup> In the present study, the hydro-methanolic extract of *A. ursinum* at a dose of 160 mg/kg exhibited the most pronounced hypoglycemic effect in diabetic mice, outperforming both ginger and garlic at their effective dose of 500 mg/kg.

One possible reason for the difference in therapeutic doses between *A. ursinum* and ginger could be variations in the phytochemical composition of their respective extracts,

which warrants further investigation. Moreover, since the hydro-methanolic extract of *A. ursinum* did not exhibit toxic effects on the liver and kidney tissues of treated mice at the therapeutic dose, it may present a promising option for diabetes treatment.

A 2010 study by Roghani et al. found that *Allium schoenoprasum*, a member of the *Allium* family, possesses anti-diabetic properties similar to those of *A. ursinum*.<sup>25</sup> In another study, Ikechukwu et al. reported that the ethanol extract of *A. cepa* (onion) at a dose of 25 mg/kg significantly reduced blood glucose levels within 24 hours of oral administration. These therapeutic effects may be attributed to the presence of bioactive compounds such as quercetin, S-methyl cysteine sulfoxide, allyl propyl disulfide, and polyphenols, which can enhance glucose uptake in peripheral tissues, improve insulin sensitivity by modulating NADP<sup>+</sup>/NADPH function, and stimulate pancreatic  $\beta$ -cell regeneration.<sup>26</sup>

Since bioactive compounds such as methyl-2-propenyl disulfide and propenyl propyl disulfide have also been identified in *A. ursinum* extract, it is plausible that this plant may similarly contribute to pancreatic  $\beta$ -cell regeneration, akin to *A. cepa*. To explore this hypothesis, we investigated the metabolites present in plasma.

Reports indicate that the leaves and bulbs of *A. ursinum* contain numerous phenolic compounds and high concentrations of thiopolysulfides — a group of organic sulfur compounds characteristic of all *Allium* species. The methanol-soluble and aqueous fractions of the leaves exhibit strong antioxidant capacity; however, this activity varies significantly depending on the extraction method and the geographical origin of the plant material. *A. ursinum* (particularly its leaves) demonstrates pronounced anti-inflammatory and antibacterial properties. The bioactive constituents of wild garlic are capable of inhibiting the growth of pathogenic bacteria and modulating cytokine release in cells exposed to inflammatory stimuli. Moreover, the thiopolysulfides present in the plant markedly suppress the proliferation of cancer cell lines and display a selective cytotoxic effect, with minimal impact on non-cancerous tissue cells.<sup>16</sup>

To identify the metabolites involved in blood glucose reduction, the present study investigated serum metabolic changes in mice treated with *A. ursinum* extract using <sup>1</sup>HNMR spectroscopy.

The major altered metabolites included NADH, hydroxocobalamin, citric acid, acetoacetic acid, carbon dioxide, L-glutamic acid, 3-hydroxybutyric acid, and pyruvic acid. Notably, the metabolite succinate, involved in the synthesis and degradation of ketone bodies, and 3-hydroxybutyrate, a key component of the ketone body cycle, exhibited significant changes in diabetic mice treated with *A. ursinum* extract compared to the control group. Succinate

and 3-hydroxybutyrate, both essential ketone bodies, play a crucial role in reducing glucose consumption and providing energy to various tissues, particularly the brain, during periods of glucose deficiency.<sup>27</sup>

Jain et al.<sup>28</sup> reported that hydroxybutyric acid metabolites can induce oxidative stress in endothelial cells by stimulating lipid peroxidation and generating reactive oxygen species (ROS). This mechanism may explain why individuals with diabetes are more prone to developing cardiovascular diseases associated with vascular damage. In our study, administration of *A. ursinum* extract reduced hydroxybutyric acid levels in diabetic mice, suggesting that this extract may help mitigate diabetes-related vascular damage.

Giugliano et al. and Baynes et al.<sup>29,30</sup> demonstrated that elevated lipid peroxide levels in diabetic patients' blood may result from an increase in free radicals, which are produced as byproducts of glycation and glucose oxidation. Furthermore, studies have shown that cellular defense mechanisms against oxidative stress can lead to membrane dysfunction through lipid peroxidation and the accumulation of malondialdehyde (MDA).

Mitchell et al.<sup>31</sup> conducted a study on the medical aspects of ketone body metabolism, revealing that pathological causes of ketosis include diabetes, childhood hypoglycemic ketosis, corticosteroid use, and alcohol consumption. Their findings also highlighted that the absence of ketosis in patients with abnormal hypoglycemia is a distinguishing factor. These observations align with our metabolic pathway analysis, which showed increased ketone body metabolism in diabetic mice compared to the negative control group.

Another notable metabolic alteration observed in diabetic mice treated with *A. ursinum* extract was a reduction in NADH levels. NAD<sup>+</sup> is a crucial molecule in metabolism and redox signaling, and its balance with NADH plays a fundamental role in cellular homeostasis. In diabetes and its complications, this balance is often severely disrupted. Hyperglycemia promotes excessive NADH production through glycolysis and the Krebs cycle, while NAD<sup>+</sup> levels can be depleted due to the overactivation of the poly-ADP-ribose polymerase (PARP) pathway, which utilizes NAD<sup>+</sup> as a substrate.<sup>32</sup>

Our findings indicate that *A. ursinum* extract effectively reduced NADH levels, potentially helping to restore redox balance. Additionally, dysfunctions in lactate dehydrogenase (LDH) activity in red blood cells and complex I impairment in mitochondria can contribute to NADH accumulation and NAD<sup>+</sup> deficiency. An imbalance in the NADH/NAD<sup>+</sup> redox state leads to oxidative stress and subsequent oxidative damage to macromolecules such as DNA, lipids, and proteins.<sup>33,34</sup> Consequently, oxidative damage caused by redox imbalance is considered a key factor in the onset and progression of diabetes and its complications.

Pyruvate is another metabolite significantly altered in diabetes, and in our study, its levels were elevated in diabetic mice. As a crucial intermediate in cellular metabolism, pyruvate plays a central role in multiple metabolic pathways, including the pyruvate metabolism pathway, arginine and proline metabolism, the Krebs cycle, glycine-serine-threonine metabolism, tyrosine metabolism, alanine-aspartate-glutamate metabolism, and the glyoxylate and dicarboxylate cycle. Pyruvate is primarily generated as the final product of glycolysis, where pyruvate kinase catalyzes the conversion of phosphoenolpyruvate to pyruvate. Additionally, lactate from the LDH pathway and alanine from the ALT pathway serve as important sources of pyruvate.

Mitochondrial pyruvate metabolism is tightly regulated by multiple enzymes, and mutations in genes encoding pyruvate metabolic regulators have been linked to various diseases, including cancer, heart failure, neurodegeneration, and diabetes.<sup>35</sup> In diabetes, pyruvate metabolism is disrupted across multiple organs. In the heart, dysregulation of pyruvate dehydrogenase kinase 4 (PDK4) leads to excessive fatty acid oxidation and increased reactive oxygen species (ROS) formation in mitochondria. In skeletal muscle and liver, diabetes upregulates PDK expression, resulting in pyruvate dehydrogenase (PDH) inhibition.<sup>36</sup> In the kidneys, preferential oxidation of fatty acids further inhibits PDH activity, contributing to increased ROS production and oxidative stress.

Citrate was another metabolite significantly altered in multiple metabolic pathways, including the citric acid cycle (TCA cycle), alanine-aspartate-glutamate metabolism, and the glyoxylate-dicarboxylate cycle. Citrate is synthesized through the condensation of acetyl-CoA (a two-carbon compound) and oxaloacetate (a four-carbon compound), a reaction catalyzed by citrate synthase.<sup>37</sup> Cardiovascular complications are a significant risk associated with diabetes, contributing to around 80% of diabetes-related deaths.<sup>38</sup> Citrate injection provided partial protection against diabetes-induced cardiac damage. In the present study, citrate levels increased following the administration of *A. ursinum* extract in diabetic mice, suggesting that this extract may contribute to reducing diabetes-associated tissue damage. These findings highlight the potential therapeutic role of TCA cycle activation in protecting the heart against diabetic stress. Additionally, citrate is readily available from dietary sources such as fruits and beverages, and its supplementation may also stimulate lipid metabolism. Therefore, maintaining balanced cellular citrate levels is essential for overall metabolic health.<sup>39</sup>

The study found significant changes in the experimental groups compared to the control groups for L-glutamate (Glu), a crucial metabolite involved in multiple metabolic pathways, including glutamine-glutamate metabolism, arginine-proline metabolism, alanine-aspartate-glutamate metabolism, and the glyoxylate and dicarboxylate cycle. Glutamic acid,

or its ionic form Glu, is one of the most abundant amino acids in nature, playing critical roles at both cellular and systemic levels. In the gut and liver, Glu serves as an energy source and a precursor for various biological molecules. Glu functions as an excitatory neurotransmitter within the mammalian central nervous system, interacting with specific receptors and contributing to short-term and long-term memory and learning.<sup>40</sup>

Glu metabolism is essential for the biosynthesis of nucleic acids and proteins. Deficiencies in key enzymes in this process can lead to disorders like type-2 hyperprolinemia, gyrate atrophy, hemolytic anemia, 5-oxoprolinuria, and hyperammonemia. Studies suggest that cell death, potentially due to Glu toxicity, is an early consequence of diabetes.<sup>41</sup> Moreover, elevated Glu levels in the vitreous fluid of diabetic patients have been implicated in the early stages of diabetic retinopathy. Additionally, 3-propane tricarboxylate, a metabolite involved in the Krebs cycle, was found to be altered in diabetic patients. This metabolite functions as an inhibitor of the enzyme aconitase, thereby disrupting the Krebs cycle and contributing to metabolic dysfunction in diabetes.

These metabolites play a key role in cellular energy homeostasis, directly participating in pathways of energy production and consumption, including glycolysis, the Krebs cycle, and ketogenesis. These processes are essential for the regulation of glucose balance and overall cellular energy. The observed alterations in NADH, pyruvate, and citric acid levels suggest that the extract likely exerts a direct influence on oxidative metabolism and glucose utilization, thereby contributing to its hypoglycemic effect. Additionally, the elevated levels of metabolites such as 3-hydroxybutyrate and acetic acid point to the activation of fatty acid oxidation pathways and a shift in energy substrate utilization, a response to the reduction in blood glucose levels.

Taken together, these findings suggest that some of the metabolic changes are directly induced by the active compounds in the extract, such as enhanced glucose consumption and TCA cycle activation. In contrast, other changes appear to represent compensatory metabolic adaptations to lower blood glucose, such as the increased production of ketone bodies to sustain energy balance. The interplay between these direct and compensatory metabolic alterations ultimately underpins the observed hypoglycemic effect.

## Conclusion

The hydro-methanolic extract of *A. ursinum* effectively reduced blood glucose levels in diabetic mice by influencing key metabolic pathways such as ketone body metabolism, glycolysis/gluconeogenesis, and the citrate cycle. NMR-based metabolomic analysis revealed critical alterations in endogenous metabolites associated with this hypoglycemic

effect. These findings not only emphasize the therapeutic potential of *A. ursinum* as a natural antidiabetic agent but also highlight the value of metabolite profiling in elucidating its biochemical mechanisms. The glucose-lowering metabolites identified in this study could be promising targets for the development of future antidiabetic treatments.

### Authors' Contributions

TE conceptualized the study, developed the methodology, collected the data, performed formal analysis, and wrote the original draft of the manuscript; MA supervised the study, analyzed the data, and critically reviewed the manuscript; ZR and FR curated the data, performed statistical analysis, and interpreted the results; ZP and SA contributed to the literature review, visualized the data, and assisted with manuscript editing. All authors read and approved the final manuscript.

### Ethical Approval

The Ethics Committee of the Islamic Azad University, Babol Branch, Iran, reviewed and approved the study protocol (approval code: IR.IAU.BABOL.REC.1400.018). All animal experiments were conducted following the approved methods established by the Ethics Committee of the Islamic Azad University, Babol Branch.

### Conflict of Interest Disclosures

The authors declare that they have no conflicts of interest.

### Acknowledgment

We would like to thank the Research and Technology Comprehensive Laboratory of Baqiyatallah University of Medical Sciences for their guidance and support.

### References

- Zakir M, Ahuja N, Surksha MA, Sachdev R, Kalariya Y, Nasir M, et al. Cardiovascular Complications of Diabetes: From Microvascular to Macrovascular Pathways. *Cureus*. 2023 24;15(9):45835. doi:10.7759/cureus.45835
- Caturano A, D'Angelo M, Mormone A, Russo V, Mollica MP, Salvatore T, et al. Oxidative stress in type 2 diabetes: impacts from pathogenesis to lifestyle modifications. *Curr Issues Mol Biol*. 2023;45(8):6651-66. doi:10.3390/cimb45080420
- Cojocaru KA, Luchian I, Goriuc A, Antoci LM, Ciobanu CG, Popescu R, et al. Mitochondrial dysfunction, oxidative stress, and therapeutic strategies in diabetes, obesity, and cardiovascular disease. *Antioxidants*. 2023;12(3):658. doi:10.3390/antiox12030658
- Sandler, M. & Jordaan HF. Cutaneous reaction to zinc-a rare complication of insulin treatment-a case report. *South African Med J*. 1989;75(7):342-3.
- Heinzerling L, Raile K, Rochlitz H, Zuberbier T, Worm M. Insulin allergy: clinical manifestations and management strategies. *Allergy*. 2008;63(2):148-55. doi:10.1111/j.1398-9995.2007.01567.x
- Bombicz M, Prikosz D, Varga B, Gesztelyi R, Kertesz A, Lengyel P, et al. Anti-atherogenic properties of *allium ursinum* liophyllisate: Impact on lipoprotein homeostasis and cardiac biomarkers in hypercholesterolemic rabbits. *Int J Mol Sci*. 2016;17(8):1284. doi:10.3390/ijms17081284
- Preuss HG, Clouatre D, Mohamadi A, Jarrell ST. Wild garlic has a greater effect than regular garlic on blood pressure and blood chemistries of rats. *Int Urol Nephrol*. 2001;32(4):525-30. doi:10.1023/A:1014417526290
- Emami F, Naghsh Tabrizi B. Evaluation the effect garlet tablet on serum lipid profile. *Avicenna J Clin Med*. 2006;13(2):37-40.
- Roghani ME, Baluchnejadmojarad TO, Ogbi K. Survey the effect of feeding of *Allium Latifolium* on contractile reactivity of aorta of diabetic rats. *J Guilan Univ Med Sci*. 2008;17(65):1-6.
- Ivanova A, Mikhova B, Najdenski H, Tsvetkova I, Kostova I. Chemical composition and antimicrobial activity of wild garlic *Allium ursinum* of Bulgarian origin. *Nat Prod Commun*. 2009;4(8):1934578X0900400808.
- Nagana Gowda G, Zhang S, Gu H, Asiago V, Shanaiah N, Raftery D. Metabolomics-based methods for early disease diagnostics: A review. *Expert Rev of Mol Diagn*. 2008;8:617-33
- Puchades-Carrasco L, Pineda-Lucena A. Metabolomics applications in precision medicine: an oncological perspective. *Curr Top Med Chem*. 2017;17(24):2740-51. doi:10.2174/1568026617666170707120034
- Hajjaliani F, Shahbazzadeh D, Maleki F, Elmi T, Tabatabaie F, Zamani Z. the metabolomic profiles of sera of mice infected with *plasmodium berghei* and treated by effective fraction of *naja naja oxiana* using 1H nuclear magnetic resonance spectroscopy. *Acta Parasitol*. 2021;66(4):1517-27. doi:10.1007/s11686-021-00456-7
- Elmi T, Ardestani MS, Hajjaliani F, Motevalian M, Mohamadi M, Sadeghi S, et al. Novel chloroquine loaded curcumin based anionic linear globular dendrimer G2: A metabolomics study on *Plasmodium falciparum* in vitro using 1H NMR spectroscopy. *Parasitology*. 2020;147(7):747-59. doi:10.1017/S0031182020000372
- Elmi T, Gholami S, Azadbakht M, Rahimi-Esboei B, Geraili Z. The effects of hydroalcoholic extract of leaves and onion of *Allium paradoxum* on *Giardia lamblia* in mice. *J Shahrekord Univ Med Sci*. 2014;16(5).
- Khanabadi F, Badirzadeh A, Kalantari Hesari A, Akbariqomi M, Torkashvand H, Didehdar M, et al. In Vivo Anti-malarial Activity and Toxicity Studies of *Allium ursinum* (Wild Garlic) Hydroalcoholic Extract. *J Appl Biotechnol Rep*. 2022;9(3):781-9. doi:10.30491/jabr.2022.344903.1538
- Huang ZR, Zhao LY, Zhu FR, Liu Y, Xiao JY, Chen ZC, et al. Anti-diabetic effects of ethanol extract from *Sanguangporous vaninii* in high-fat/sucrose diet and streptozotocin-induced diabetic mice by modulating gut microbiota. *Foods*. 2022;11(7):974. doi:10.3390/foods11070974
- Elmi T, Ardestani MS, Motevalian M, Hesari AK, Hamzeh MS, Zamani Z, et al. Antiplasmodial effect of nano dendrimer G2 loaded with chloroquine in mice infected with *plasmodium berghei*. *Acta Parasitol*. 2022;67(1):298-308. doi:10.1007/s11686-021-00459-4
- Lai KC, Kuo CL, Ho HC, Yang JS, Ma CY, Lu HF, et al. Diallyl sulfide, diallyl disulfide and diallyl trisulfide affect drug resistant gene expression in colo 205 human colon cancer cells in vitro and in vivo. *Phytomedicine*. 2012;19(7):625-30. doi:10.1016/j.phymed.2012.02.004
- Sobolewska D, Podolak I, Makowska-Wąs J. *Allium ursinum*: botanical, phytochemical and pharmacological overview. *Phytochem Rev*. 2015;14(1):81-97. doi:10.1007/s11101-013-9334-0
- Štajner D, Popović BM, Čanadanović-Brunet J, Štajner M.

- Antioxidant and scavenger activities of *Allium ursinum*. *Fitoterapia*. 2008;79(4):303-5. doi:10.1016/j.fitote.2007.01.008
22. Tudu CK, Dutta T, Ghorai M, Biswas P, Samanta D, Oleksak P, et al. Traditional uses, phytochemistry, pharmacology and toxicology of garlic (*Allium sativum*), a storehouse of diverse phytochemicals: A review of research from the last decade focusing on health and nutritional implications. *Front Nutr*. 2022;9:949554. doi:10.3389/fnut.2022.929554
  23. Sendl A. *Allium sativum* and *Allium ursinum*: Part 1 Chemistry, analysis, history, botany. *Phytomedicine*. 1995;1(4):323-39. doi:10.1016/S0944-7113(11)80011-5
  24. Fadil HK, Yousef KM. Effect of garlic and ginger extracts on the levels of glucose and Peptide-c in diabetic mice. *J Agric Environ Vet Sci*. 2021;5(4):105-19.
  25. Roghani ME, Khalili MO, Aghaie M, Ansari FB, Sharayeli MB. Effect of oral feeding of *Allium schoenoprasum* L. on blood glucose and lipid level in diabetic Rats. *J Gorgan Univ Med Sci*. 2010;12(1):9-14.
  26. J Ikechukwu O, S Ifeanyi O. The antidiabetic effects of the bioactive flavonoid (kaempferol-3-O-β-D-6 {P-Coumaroyl} glucopyranoside) isolated from *Allium cepa*. *Recent Pat Antiinfect Drug Discov*. 2016;11(1):44-52.
  27. Laffel L. Ketone bodies: a review of physiology, pathophysiology and application of monitoring to diabetes. *Diabetes Metab Res Rev*. 1999;15(6):412-26. doi:10.1002/(SICI)1520-7560(199911/12)15:6<412::AID-DMRR72>3.0.CO;2-8
  28. Jain SK, Kannan K, Lim G. Ketosis (acetoacetate) can generate oxygen radicals and cause increased lipid peroxidation and growth inhibition in human endothelial cells. *Free Radic Biol Med*. 1998;25(9):1083-8. doi:10.1016/S0891-5849(98)00140-3
  29. Giugliano D, Ceriello A, Paolisso G. Oxidative stress and diabetic vascular complications. *Diabetes Care*. 1996;19(3):257-67. doi:10.2337/diacare.19.3.257
  30. Baynes JW. Role of oxidative stress in development of complications in diabetes. *Diabetes*. 1991;40(4):405-12. doi:10.2337/diab.40.4.405
  31. Mitchell GA, Kassoovska-Bratinova S, Boukaftane Y, Robert MF, Wang SP, Ashmarina L, et al. Medical aspects of ketone body metabolism. *Clinical and investigative medicine*. *Clin Invest Med*. 1995;18(3):193-216.
  32. Wu J, Jin Z, Zheng H, Yan LJ. Sources and implications of NADH/NAD<sup>+</sup> redox imbalance in diabetes and its complications. *Diabetes Metab Syndr Obes: Targets Ther*. 2016;145-53. doi:10.2147/DMSO.S106087
  33. Teodoro JS, Rolo AP, Palmeira CM. The NAD ratio redox paradox: why does too much reductive power cause oxidative stress?. *Toxicol Mech Methods*. 2013;23(5):297-302. doi:10.3109/15376516.2012.759305
  34. Yan LJ. Pathogenesis of chronic hyperglycemia: from reductive stress to oxidative stress. *J Diabetes Res*. 2014;2014(1):137919. doi:10.1155/2014/137919
  35. Gray LR, Tompkins SC, Taylor EB. Regulation of pyruvate metabolism and human disease. *Cell Mol Life Sci*. 2014;71(14):2577-604. doi:10.1007/s00018-013-1539-2
  36. Chambers KT, Leone TC, Sambandam N, Kovacs A, Wagg CS, Lopaschuk GD, et al. Chronic inhibition of pyruvate dehydrogenase in heart triggers an adaptive metabolic response. *J Biol Chem*. 2011;286(13):11155-62. doi:10.1074/jbc.M110.217349
  37. Akram M. Citric acid cycle and role of its intermediates in metabolism. *Cell Biochem Biophys*. 2014;68(3):475-8. doi:10.1007/s12013-013-9750-1
  38. Martín-Timón I, Sevillano-Collantes C, Segura-Galindo A, del Cacizo-Gymez FJ. Type 2 diabetes and cardiovascular disease: have all risk factors the same strength?. *World J Diabetes*. 2014;5(4):444-70. doi:10.4239/wjd.v5.i4.444
  39. Kay J, Weitzman PDJ, editors. *Krebs citric acid cycle: half a century and still turning*. *Biochem Soc Symp*. 1987.
  40. Albarracín SL, Baldeyn ME, Sangronis E, Cucufate Petruschina A, Reyes FG. L-Glutamato: un aminoácido clave para las funciones sensoriales y metabólicas. *Arch Latinoam Nutr*. 2016;66(2):101-12.
  41. Gowda K, Zinnanti WJ, LaNoue KF. The influence of diabetes on glutamate metabolism in retinas. *J Neurochem*. 2011;117(2):309-20. doi:10.1111/j.1471-4159.2011.07206.x